FLORE
Repository istituzionale dell'Università degli Studi di Firenze

Development of a brake by wire system design for car stability controls

Questa è la Versione finale referata (Post print/Accepted manuscript) della seguente pubblicazione:

Original Citation:

Development of a brake by wire system design for car stability controls / Montani, M., Capitani, R., Annicchiarico, C.. - In: PROCEDIA STRUCTURAL INTEGRITY. - ISSN 2452-3216. - ELETTRONICO. - 24:(2019), pp. 137-154. [10.1016/j.prostr.2020.02.013]

Availability:

The webpage https://hdl.handle.net/2158/1184580 of the repository was last updated on 2020-02-25T09:26:15Z

Published version:

DOI: 10.1016/j.prostr.2020.02.013

Terms of use:

Open Access

La pubblicazione è resa disponibile sotto le norme e i termini della licenza di deposito, secondo quanto stabilito dalla Policy per l'accesso aperto dell'Università degli Studi di Firenze (https://www.sba.unifi.it/upload/policy-oa-2016-1.pdf)

Publisher copyright claim:

La data sopra indicata si riferisce all'ultimo aggiornamento della scheda del Repository FloRe - The above-mentioned date refers to the last update of the record in the Institutional Repository FloRe

(Article begins on next page)

16 October 2026

Available online at www.sciencedirect.com

ScienceDirect

Structural Integrity Procedia 00 (2019) 000–000

Structural Integrity Procedia

www.elsevier.com/locate/procedia

AIAS 2019 International Conference on Stress Analysis

Development of a brake by wire system design for car stability controls

Margherita Montani[a,*], Renzo Capitani[a], Claudio Annicchiarico[b]

[a]*Università degli Studi di Firenze-Dipartimento di Ingegneria Industriale, via di Santa Marta 3, 50139, Firenze, Italy*
[b]*Meccanica 42 s.r.l., via Madonna del Piano 6, 50019 Sesto Fiorentino (FI), Italy*

Abstract

The paper presents the development of a vehicle stability control system that is able to operate in real time, ensuring to enhance vehicle dynamics and safety in all vehicle motion conditions, even at limit of handling. The commercial cars have an Electronic Stability System, ESC,that acts actuating the brakes autonomously to correct the vehicle dynamics at limit of adhesion conditions. In this study it will be shown how the stability control system proposed can operate autonomously and constantly during vehicle motion, thanks to a controller based on a simplified vehicle model and a brake unit that operates in continuous.

The control system consists of a high-level control and four Brake-By-Wire actuators. The high-level control is an Linear Quadratic Regulator, LQR, that ensures to stabilize the yaw rate and the side slip angle minimizing the errors between the actual car values and the values given by a steady state dynamic reference model. To reach this aim the LQR gives the values of longitudinal forces that each wheel has to achieve. These values of force are sent by a CAN signal to the Cornering Brake Actuators, CBA, that with their own logic and proximity to the wheels ensure a vary fast actuation, stabilizing the vehicle and providing safety.

To validate the control system a series of manoeuvres have been carried out on a case-study test bench, that has been installed on a static driving simulator equipped with a concurrent real-time machine, the complete vehicle network and the full steering system. The control system has been design to be used as a stability system on commercial cars, requiring of common vehicle sensors, ensuring better performances and stability even in driving at limit of adhesion conditions, but also to be installed in an autonomous vehicle being able to act independently from the driver.

© 2019 The Authors. Published by Elsevier B.V.
This is an open access article under the CC BY-NC-ND license (http://creativecommons.org/licenses/by-nc-nd/4.0/)
Peer-review line: Peer-review under responsibility of the AIAS2019 organizers.

Keywords: ESP; LQR; stability control; vehicle; Brake-By-Wire; brake actuator.

1. Introduction

In the last fifty years with the increase of the electronic components on vehicles, the automotive industries have invested in development of stability control systems to ensure passenger safety. Nowadays, in commercial cars, sta-

* Corresponding author. Tel.: +39-055-275-8707.
E-mail address: margherita.montani@unifi.it

2210-7843 © 2019 The Authors. Published by Elsevier B.V.
This is an open access article under the CC BY-NC-ND license (http://creativecommons.org/licenses/by-nc-nd/4.0/)
Peer-review line: Peer-review under responsibility of the AIAS2019 organizers.

bility is ensured by the action of the Electronic Stability Program, ESP, a device which is currently able to correct the vehicle dynamic at limit of adhesion conditions(van Zanten et al.). However the common ESP is not able to allow the proper stability and therefore the achievement of the best dynamic performances at every time during vehicle motion.

The vehicle dynamic is strongly non-linear and usually needs a high computational cost to be controlled. In commercial vehicle, the Brake-By-Wire system used by the ESP to correct vehicle behaviour has a single central logic control and hydraulic lines to actuate the calipers; this architecture involves a certain amount of delay between command and actuation. A structure with an high-level control system, composed by a Linear Quadratic Regulator,LQR, and four single wheel actuators with its own low actuation logic, ensures a reduction of the delays, real time operation and improve safety.

The high-level control task is to make the vehicle follow a reference behaviour. This behaviour is provided by a reference model using steady state yaw rate and side slip angle formulations. Tracking the errors between reference and actual values of the yaw rate and side slip angle the controller is able in real time to provide at the brake actuators the pressure values that ensure these errors are close to zero. This configuration is able to increase the system responsiveness and its accuracy, achieving them with the reduction of the inertia related to each caliper and the possibility of continuously tracking four different pressure targets, additionally the reliability is improved: being inherently redundant, if one actuator goes to fault conditions, the others can ensure the safety of the brake plant.

The yaw rate and side-slip angle are chosen as states of control because of their capability to detect the vehicle instability. The yaw rate is the angular velocity with which the vehicle moves around yaw axis. Its value is given by a standard Inertial Measurement Unit, IMU, already available in all commercial vehicles. The side slip angle, is the angle between the direction of the vehicle velocity and the longitudinal barycentric axis of the car. For this application a new architecture was developed by Novi et al. (2016). In this study a Neural Network was trained with vehicle inertial values, longitudinal, lateral accelerations and yaw rate, given by the low cost IMU sensor, that can be able to estimate in real time the side-slip angle trend (Melzi et al. (2011)-Du et al. (2010)). Then a non-linear state observer,Unscented Kalman Filter, UKF, was added to improve the network estimation extending the data domain(Boada et al. (2016)-Li et al. (2014)). This type of architecture has allowed to decrease the computational time, having a real-time measurement of side slip angle, and to decrease the economic cost, not using more sophisticated sensors.

In the state of the art different typologies of vehicle stability control can be found. Because of the great non-linearity of dynamic vehicle many authors, as Ataei et al. (2019), Falcone et al. (2008),Falcone et al. (2007), Jalali et al. (2017) and Barbarisi et al. (2009) chose to implement a Non-linear Model Predictive Control (NMPC), that is able to take into account the non-linearities, the mutual interaction of each dynamic states and the possibility of using constraints for both the states and inputs. The main problem of this type of control is the computational cost that precludes real-time usage. For this reason, other authors, Zhu et al. (2016) and Ohno et al. (1994), proposed to use Neural Network, capable of reproducing the vehicle dynamics and acts in real time reducing computational cost. However, this type of control is based on an end-to-end approach, without any analytic correlation with the dynamics of the system. It will be critical for the safety assessment of the control system, because it can't ensure the robustness of control under each dynamic conditions. Then, a LQR, lean and easy to implement, was chosen. It permits an optimal control of the dynamic model and a robust control thanks to precise representation of the vehicle dynamics. Compared to the state of the art, the authors as Dal Poggetto et al. (2016) and Li et al. (2015), use an LQR that acts leading the side-slip angle and the yaw rate under a saturation limit. This system can help to keep the vehicle safe but doesn't allow it to achieve the dynamic performance available. Instead, it is useful to have continuous control over the state values and to implement an LQR capable of tracing a variant time reference model which continuously provides on-line the target yaw rate and side slip angle and therefore the errors that must be minimized by exploiting the possibilities of the brake actuators. In this way, the onset of instability is prevented and a control delay between the upper controller and the pressure controllers is not leaded.

To validate the control system, the results achieved on a static driver simulator, equipped by single wheel brake actuator and a car real-time complex multi-body model built up with the Vi-Grade software, are shown.

Nomenclature

m	vehicle mass

u	vehicle longitudinal velocity
v	vehicle lateral velocity
β	vehicle side slip angle
r	vehicle yaw rate
F_{xij}	longitudinal force at the front/rear-left/right wheel
F_{yij}	lateral force at the front/rear-left/right wheel
δ	front steering wheel anlge
I	vehicle inertia
$I_{\omega ij}$	front/rear-left/right wheel inertia
ω_{ij}	front/rear-left/right wheel angular velocities
M_{bij}	front/rear-left/right wheel braking torque
P_{bij}	front/rear-left/right wheel braking pressure
C_{yi}	front/rear slip angle
α_i	front/rear slip angle
a_i	front/rear wheelbase
Δ_{ij}	understeering gradient
A_c	cylinder section
R	wheel radius
μ	contact grip

2. Reference Model

During a manoeuvre, lateral and yawing dynamics of the vehicle change over time according to initial condition, steering wheel angle and longitudinal velocity imposed by the driver. To extrapolate the inner characteristics of the vehicle and be able to act the brakes to compensate the understeering, or the oversteering behaviour of the vehicle, the steady state values of the yaw rate and side slip angle are calculated.

The understeering gradient, Δ, is the difference between actual and kinematic steering. Δ is calculated as gradient to lateral acceleration of the difference between front and rear wheel slip angles. In this way, the yaw rate of the vehicle can be expressed as a function of the vehicle parameters (shown in table 1), of the cornering stiffness and of the driver's inputs, steering and speed (1-3).

Table 1.

Vehicle Parameters	Quantities
a_1	1.315 (m)
a_2	1.505 (m)
m	1751 (kg)

The steady-sate values of the side-slip angle can be estimated by the understeering gradient too, using the linearized congruence equations (4).

$$\alpha_f = \frac{m \cdot a_2 \cdot r \cdot u}{L \cdot C_{yf}}; \alpha_r = \frac{m \cdot a_1 \cdot r \cdot u}{L \cdot C_{yr}} \tag{1}$$

$$\delta = \alpha_f - \alpha_r = \frac{m}{L} \cdot \left(\frac{a_2}{C_{yf}} - \frac{a_1}{C_{yr}} \right) \cdot r \cdot u \tag{2}$$

$$\Delta = \frac{m}{L} \cdot \left(\frac{a_2}{C_{yf}} - \frac{a_1}{C_{yr}} \right) \cdot r \cdot u \tag{3}$$

$$\alpha_2 = -\beta + \frac{r \cdot a_2}{u} \tag{4}$$

$$r_s = \frac{u}{L + u^2 \cdot \Delta} \cdot \delta; \;\; \beta_s = \frac{a_2 - \dfrac{m \cdot a_1 \cdot u^2}{L \cdot C_{yr}}}{L + u^2 \cdot \Delta} \cdot \delta \tag{5}$$

The yaw rate and the side slip angle estimated by equations (5) are the values that the vehicle has to follow in order to ensure steady behaviour.

On the other hand, these expressions don't ensure to consider the limit of adhesion of the wheels and must be saturated to upper limits (6). In this way, the reference model is implemented to provide the yaw rate and the side-slip angle knowing the steering angle and the longitudinal velocity, ensuring that the vehicle remains in conditions of grip and handling. The logic used is given in (7).

$$r_{up} = \frac{\mu \cdot g}{u}; \beta_{up} = tan^{-1} \left(0.02 \cdot \mu \cdot g \right) \tag{6}$$

$$|r_d| = min \left(r_s, r_{up} \right); \; |\beta_d| = min \left(\beta_s, \beta_{up} \right) \tag{7}$$

Since these reference values change while the vehicle is in motion, to be able to implement them in the control, they are represented in a state-space form. It's possible to do this defining the gradients of r_s and β_s in the Laplace transform derivative, where s=1 and τ_i=0.1:

$$\dot{r_s} = \frac{r_s \cdot s}{1 + \tau_r \cdot s}; \dot{\beta_s} = \frac{\beta_s \cdot s}{1 + \tau_\beta \cdot s} \tag{8}$$

This transfer functions represent the dynamic model used by the controller to track the vehicle behaviour.

3. Vehicle optimal control mode

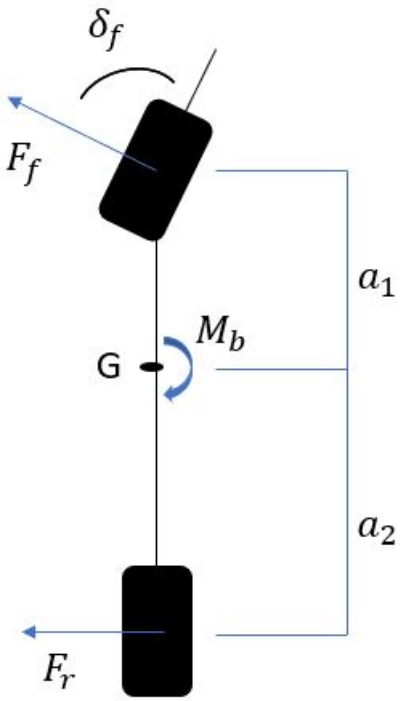

Fig. 1. Single-track-model.

The choice to use an optimal controller requires to define a vehicle dynamic model where the correlation between sates and inputs are linearized at each time step (9-10).

$$\dot{X} = AX + BY \tag{9}$$

$$Y = CX + DY \tag{10}$$

To ensure this aim, a single-track-model of vehicle with 2 degree of freedom, lateral and yaw, was implemented (Fig.1). The dynamic is expressed by the equations shown in (11-12), where the brake forces, that has to control the vehicle, are defined as a total yaw moment added in the yaw moment balance equation.

$$m \cdot \left(\dot{\beta} \cdot u + r \cdot u\right) = F_{yf} + F_{yr} + F_{xf} \tag{11}$$

$$I \cdot \dot{r} = \left(F_{yf} + F_{xf}\right) \cdot a_1 - F_{yr} \cdot a_2 + M \tag{12}$$

Every time step the following hypothesis are assumed:

- constant longitudinal velocities;
- lateral forces are in linear proportional relation with the lateral slips;

so, taken congruence equations, it is possible to define the lateral forces as dependent to side slip angle and yaw rate. Tanks to this, a State-Space of the vehicle was implemented, where the states (13) are the side-slip angle and the yaw rate, and the input (14) is the total yaw moment given by the brake forces on the wheels that the actuators can ensure.

$$X = [\beta, r] \tag{13}$$

$$u = [M_{tot}] \tag{14}$$

$$A = -\begin{bmatrix} \dfrac{2C_{yf} + 2C_{yr}}{m \cdot u} & 1 + \dfrac{2C_{yf} \cdot a_1 - 2C_{yr} \cdot a_2}{m \cdot u^2} \\ \dfrac{2C_{yf} \cdot a_1 + 2C_{yr} \cdot a_2}{I} & \dfrac{2C_{yf} \cdot a_1^2 + 2C_{yr} \cdot a_2^2}{I \cdot u} \end{bmatrix} \tag{15}$$

$$B = -\begin{bmatrix} 0 \\ \dfrac{-1}{I} \end{bmatrix} \tag{16}$$

As it is possible to see on the dynamic representation model (15-16), the parameters that change during vehicle motion are the longitudinal velocity and the cornering stiffnesses. So, to ensure the correct dynamic representation of the vehicle dynamic in the LQR and the optimal controller functionality in all motion condition, every time step the LQR model is optimized on-line with the estimation of the longitudinal velocity and left and right cornering stiffness

depend on the normal wheel force and the wheel slip angle. The normal forces on each wheel are estimated with the balance at vehicle moments around y-axis and the front and rear slip angles are estimated with the equation indicated in Bernard et al. (1995).

4. LQR controller design

The problem addressed is composed by a given system $\dot{x}$=f(x,u) and a feasible trajectory (x_d), so a compensator of the form u=α(x,x_d) is been designed such that $\lim_{x\to\infty}(x - x_d) = 0$. This is known as Trajectory Tracking Problem. To design a controller capable of solving this type of problem, the vehicle model State-Space was concatenated with the reference model State-Space achieving a new dynamic model (17-20). In this way, it was possible to define the outputs as the errors between the actual and the desired values of the states. So, the goal of the control becomes find the right input to minimize these errors.

$$X = \begin{bmatrix} \beta_r & r_r & \beta_d & r_d \end{bmatrix} \tag{17}$$

$$Y = \begin{bmatrix} \beta_r - \beta_d & r_r - r_d \end{bmatrix} = \begin{bmatrix} e_\beta & e_r \end{bmatrix} \tag{18}$$

$$A = \begin{bmatrix} A_r & 0 \\ 0 & A_d \end{bmatrix}; B = \begin{bmatrix} B_d \\ B_r \end{bmatrix} \tag{19}$$

$$C = \begin{bmatrix} 1 & 0 & -1 & 0 \\ 0 & 1 & 0 & -1 \end{bmatrix}; D = \begin{bmatrix} 0 \\ 0 \end{bmatrix} \tag{20}$$

Once specified the dynamic model, the control is ensured by the LQR that is an optimal linear control. This type of control uses the minimization of a quadratic cost function (21) producing the necessary gains to each state to define the value of the input (22).

$$J = \int_0^\infty (y^T Q y + u^T R u) dt \tag{21}$$

$$u = -Kx - K_d x_d \tag{22}$$

In these equations x and x_d represents respectively the model states and the reference states; u is the input, namely a total brake yaw moment; Q and R are the weigh matrices respectively for the outputs and the inputs and K is the gain matrix given by the minimization of the cost function, J, solving the Riccati equations:

$$P_k = Q + A' P_{k+1} A - A' P_{k+1} B (R + B' P_{k+1} B)^{-1} B' P_{k+1} A \tag{23}$$

$$K = (R + B' P B)^{-1} B' P A \tag{24}$$

The LQR control is, as already mentioned, an optimal control, i.e. it is optimal compared to an appropriate performance index (Mosca , 1995). This performance index is the cost function, defined in (21), whose minimization allows to solve the problem, in this case of trajectory tracking, finding the law of control in state feedback (22). Having assumed that the dynamic is steady-state, various performance indices have been resolved in relation to different longitudinal speeds and different slip conditions. Once the cornering stiffness and the longitudinal velocity are updated, the Riccati equation optimizes the cost index providing each time step the gains. At this point the control is applied in real time.

So, the controller works in two ways, one of feedback and one in forward, ensuring strength and continuous optimization.

5. Controller structure

The controller architecture, shown in the Fig. 2, is composed by a reference model, an LQR controller and a brake split logic. According to the real-time conditions, the control quantities have been discretized with a sample time of 0.001 seconds.

The reference model has the task of providing the desired values of the side-slip angle and yaw rate. It receives, as inputs, the same driver demand steering and the same longitudinal velocity of the car and thanks to the formulations shown in the model explanation section, it reproduces the vehicle behaviour and allows side slip angle and yaw rate to remain under low values and ensure stability. The LQR controller works in real-time, providing, at each time step, the correction gains to compensate the errors of the vehicle compared to the reference model. As said, to ensure that the controller works in any type of driver velocity input and dynamic condition, the cost function of the controller has to be updated each time step. So, the controller reads the longitudinal velocity of the vehicle and lateral engagement of the tires and produces the right law of control to assure the value of the yaw moment that the wheels forces have to achieve, fixing car behaviour.

The solution of the control problem is the total barycentric yaw moment that the vehicle must follow to reach the dynamic of the reference model.

To ensure that the vehicle achieves this yaw torque, a logic that splits it in pressures given to each wheel actuator was implemented. The works of this logic is to determinate which and how much the wheels are to be braked. To select the wheels, a selector based on the engagement of the wheel is made. First of all, depending on the sign of input yaw moment, it's decided which wheels between the left and right side have to be braked to compensate the error on the trajectory and linearise the vehicle behaviour to the driver's input. Then, the total yaw moment input is split between the front and rear wheels of the side selected in a proportional way: depending on the amount of lateral slip that is engaged and so on the quantity of longitudinal slip that is possible to use, the brake pressure will be bigger on the wheel with less lateral engage. In this way vehicle stabilization is ensured in all conditions of contact without running the risk of not having available to the wheel the longitudinal slip necessary to reach the yaw moment required by the controller. The percentage of moment give to each side wheel is estimated by the equation (25) and the split logic is shown in (26-29).

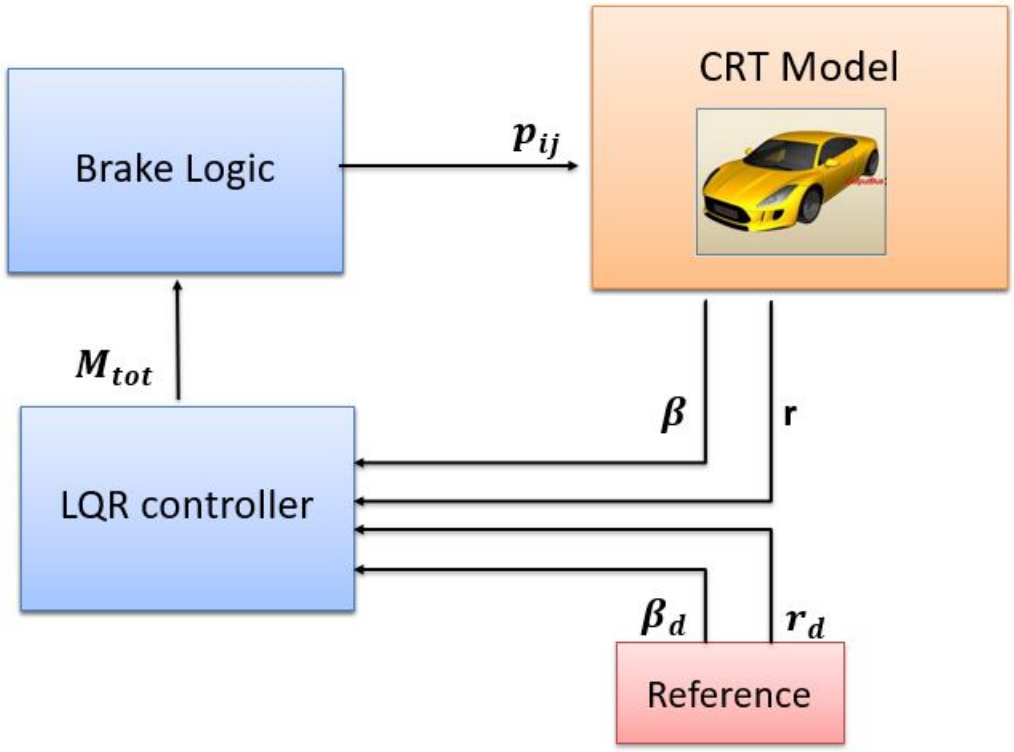

Fig. 2. controller architecture.

$$p_{fl} = \frac{F_{zfl}}{F_{zfl} + F_{zrl}}; p_{fr} = \frac{F_{zfr}}{F_{zfr} + F_{zrr}} \tag{25}$$

$$F_{xfl} = \begin{cases} 0 & M_{tot} < 0 \\ -\dfrac{|M_{tot}|\, p_{fl}}{\dfrac{t_1}{2}\cos(\delta)} & M_{tot} > 0 \end{cases} \tag{26}$$

$$F_{xrl} = \begin{cases} 0 & M_{tot} < 0 \\ -\dfrac{|M_{tot}|\left(1 - p_{fl}\right)}{\dfrac{t_2}{2}} & M_{tot} > 0 \end{cases} \tag{27}$$

$$F_{xfr} = \begin{cases} \dfrac{|M_{tot}|\, p_{fr}}{\dfrac{t_1}{2}\cos(\delta)} & M_{tot} < 0 \\ 0 & M_{tot} > 0 \end{cases} \tag{28}$$

$$F_{xrr} = \begin{cases} \dfrac{|M_{tot}|\left(p_{fr} - 1\right)}{\dfrac{t_2}{2}} & M_{tot} < 0 \\ 0 & M_{tot} > 0 \end{cases} \tag{29}$$

The forces estimated are sent to an ABS logic to ensure that the wheels don't lock up. This ABS estimates the longitudinal slip corresponding to the force wanted at each wheel and through a Lypanov control finds the pressure that ensure that the wheel achieves the desired slip value (Johansen et al., 2003). Than the estimated pressures are saturated to 100 bar, the maximum value that the brake actuators can reach.

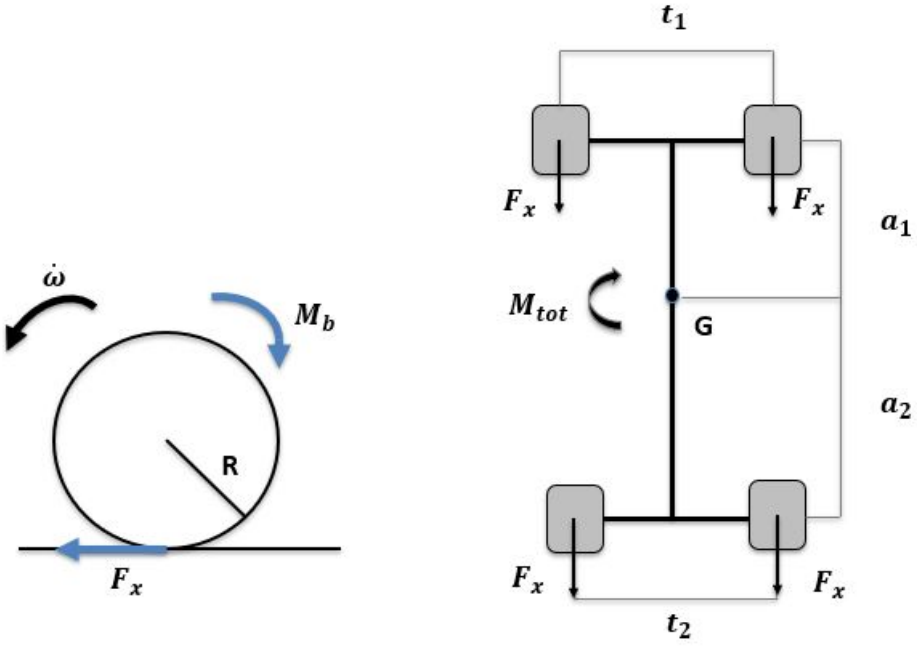

Fig. 3. (a) wheel moment equilibrium; (b) yaw moment equilibrium.

6. Driver simulator and brake actuators

The control system has been tested in a static driving simulator, putting the CBA, in the simulation loop. This allowed to consider the real performance of the brake system in tuning the controller. In detail, the brake actuators are four electro-hydraulic units, capable of building up 100 bar of braking pressure within 90 ms with the considered brake calipers.

The CBA has to be insert between the main pump and the caliper of common brake system and can be used in two modes: a manual and a By-Wire one. The driver can choose one of the two modes of operation: if the manual mode is active the brake is a standard brake with a full mechanical functionality, otherwise if the By-Wire mode is active the brake system is a CAN controlled device and the actuator can track the pressure target imposed by the high-level control system, simplifying the deployment and the integration of the whole control loop. In the event of an electronic fault, the driver can still brake mechanically, thanks to a valves system that switches to manual mode by-passing the electronic drive. Each actuator is composed of an isolated section where the ECU and the electric motor are located,

Table 2. Mechanical characteristics.

Pareameters	Values	Unit
Max. Length	0.36	(m)
Max.Height	0.13	(m)
Max. Width	0.116	(m)
Mass	3	(kg)
Max. Output Pressure (by Wire Mode)	100	(bar)
Estimated Actuation Time	0.09	(s)

and another section where the hydraulic part is involved. In this last section a piston is driven forward and backward by the electric motor thanks to a ball screw and so, it can increase and decrease the brake pressure following the target imposed by the control logic. The actuators have a very compact structure and can be easily inserted near the wheel, allowing a rapid actuation of the brake calipers and a rapid tracking of the reference dynamics, thanks to a substantial reduction of the hydraulic pipes.

Fig. 4. CBA implementation on a Static Driving Simulator.

7. Tests

To validate the control, a series of test manoeuvres was carried out to the simulator. These manoeuvres were made to bring the vehicle at limit of handling and in steady-state conditions; they are a Sine with Dwell,SWD, given by the ESC test procedure of the European normative (UN/ECE, 2015), and a steering pad.

They are close-loop manoeuvres built on car real time Vi-grade software with a sample time of 0,001 second. The characteristics of every manoeuvre are shown in the Table 3:

Table 3. Tests Configuration

Maneuvers	Longitudinal velocities	Steering amplitude	Steering frequency
SWD	80 ($\frac{km}{h}$)	270 (deg)	0.7 (Hz)
Steering PAD	100-150 ($\frac{km}{h}$)	200 (deg)	1 ($\frac{deg}{s}$)

8. Results

8.1. Steering PAD

This test is intended to assess the maximum lateral acceleration under quasi-stationary conditions that the vehicle can maintain. The manoeuvre consists in getting the vehicle to a certain longitudinal speed and then applying a steering rotation with constant angular velocities. In the graphs below the results of manoeuvres done with different velocities, 100 km/h and 150 km/h, are shown.

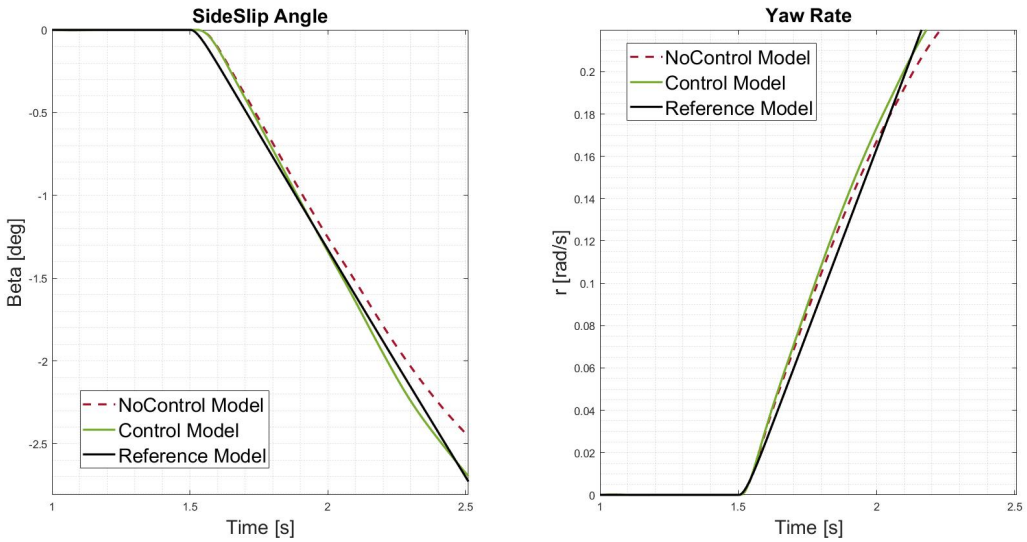

Fig. 5. Control operation in a 100 km/h Steering Pad.

Figg. 5, 6 show the trends of side slip angle and yaw rate over time at various speed, in case of uncontrolled vehicle, controlled vehicle and reference model. It's possible to see that the reference model, that represent a quasi-stationary state, has a linear trend, in which the vehicle responds to the driver's inputs in a smooth manner, ensuring good

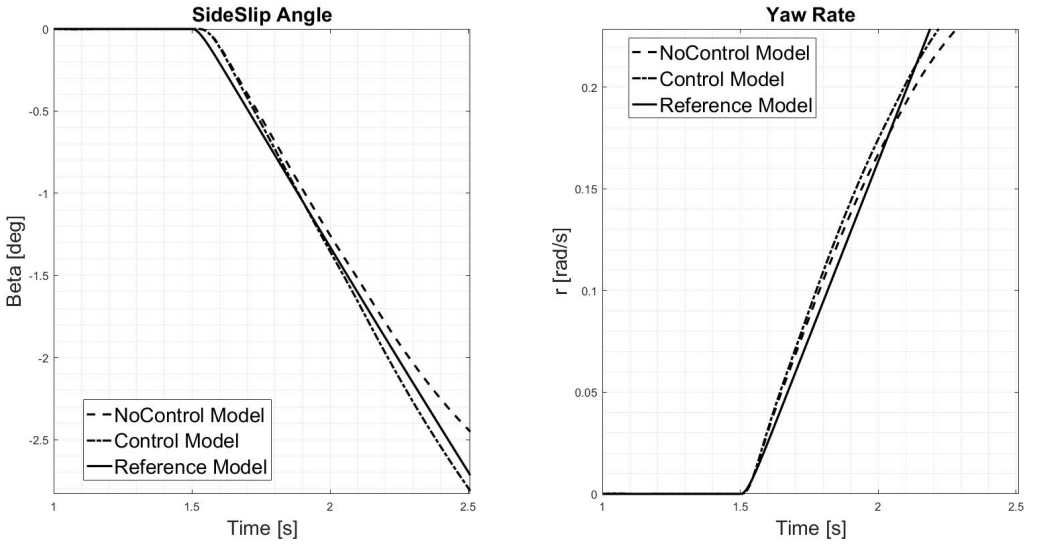

Fig. 6. Control operation in a 150 km/h Steering Pad.

handling and stability. The controlled vehicle follows the trend of the reference model ensuring better performance than an uncontrolled vehicle.

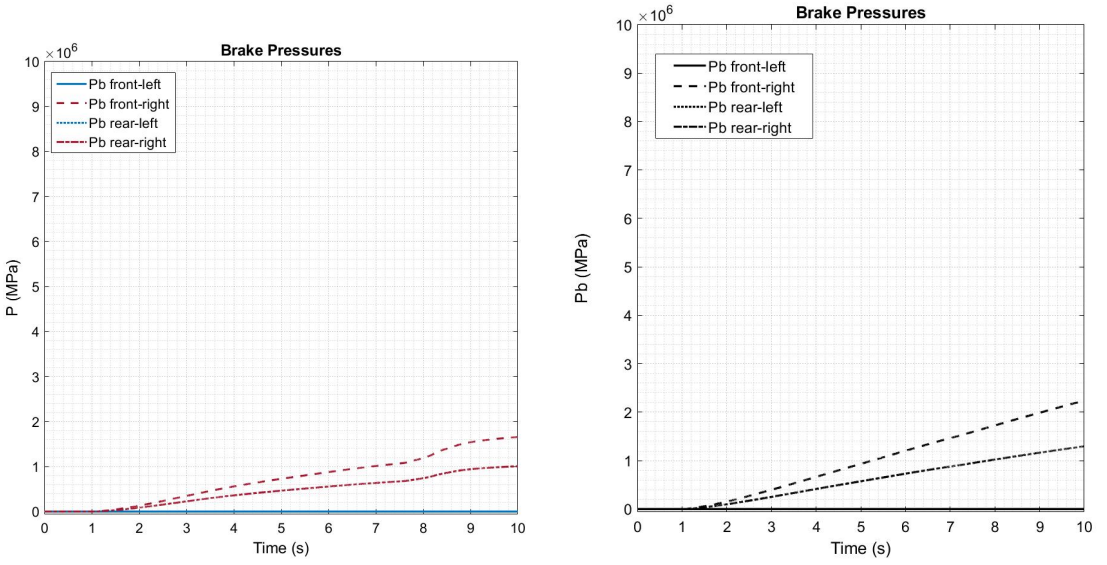

Fig. 7. (a) Braking pressures in a 100 km/h Steering Pad; (b) Braking pressures in a 144 km/h Steering Pad.

By Fig. 7, it is possible to validate the brake logic. The uncontrolled vehicle has higher values of yaw rate and side slip angle than the reference. To correct the vehicle's dynamics and make it close to steady-state behaviour, the control logic sends a pressure input to the actuators of the wheels outside the curve so as to counteract the growth of yaw rate and vehicle instability. In fact, the right wheels are actuated proportionally and a closer trajectory than the vehicle without the controller is ensured (Fig.10). As the speed increases, the brake pressure also increases to counteract the additional lateral force generated.

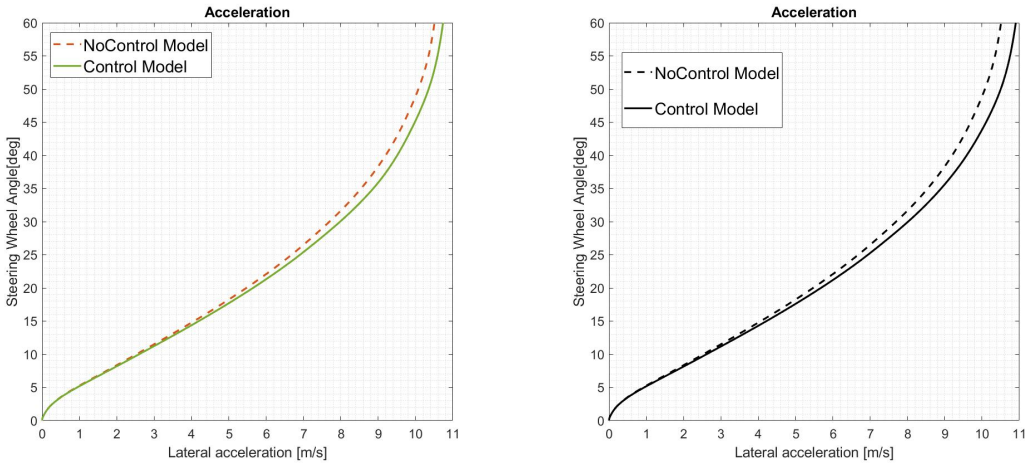

Fig. 8. (a) Steering Wheel Angle as function of Lateral Acceleration in a 100 km/h Steering Pad; (b) Steering Wheel Angle as function of Lateral Acceleration in a 144 km/h Steering Pad.

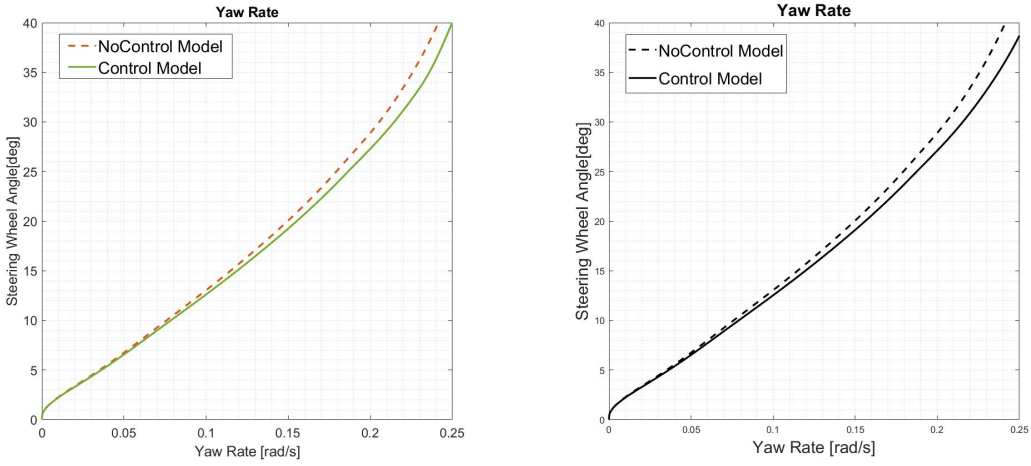

Fig. 9. (a) Steering Wheel Angle as function of Yaw Rate in a 100 km/h Steering Pad; (b) Steering Wheel Angle as function of Yaw Rate in a 144 km/h Steering Pad.

In Figg. 8, 9, instead, shows the improvement of the vehicle performances. The trend of the understeering curve (Fig.8), where the steering is given as function of lateral acceleration, illustrates that the vehicle equipped with the control in both situations can reach higher lateral acceleration and the slope of the curve is lower. This means an improvement of the performances, because the vehicle is able to maintain stability at higher accelerations and an improvement of vehicle handling, because it replies at the driver steer in more neutral way.

In the end it's shown the trend of the steering as function of the yaw rate. It's possible to note that the steer remains linear for higher values of the yaw rate. This is another index of the better levels of the car and results in the achievement of closer trajectory (Fig.10).

8.2. Sine With Dwell

This type of manoeuvre allows to verify the stability of the vehicle as it is very demanding and brings the vehicle to the limit of handling.

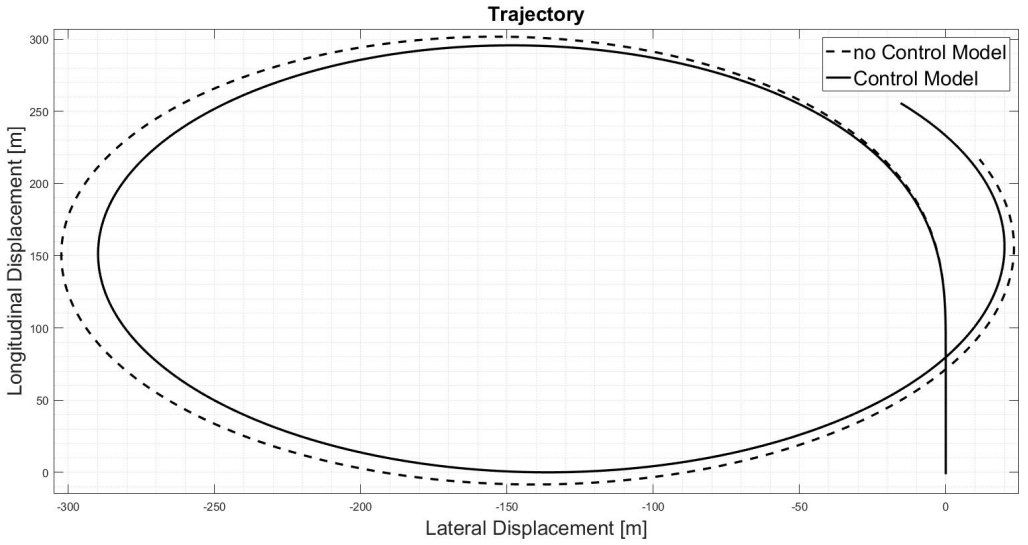

Fig. 10. Trajectory in a 100 km/h Steering Pad.

The type of test, required by the normative, involves identifying the steering angle, δ_0,at which the car achieves lateral acceleration of 0,3 g with a longitudinal speed of 80 km/h. Than another series of tests involve the SWD steering input with an increasing amplitude of $\delta = k\delta_0$, from k=1,5 to k=6,5. In this study the maximum value of the steering amplitude is 270 deg, and only the results achieved with this steering angle are shown below, as they represent the most critical driving condition.

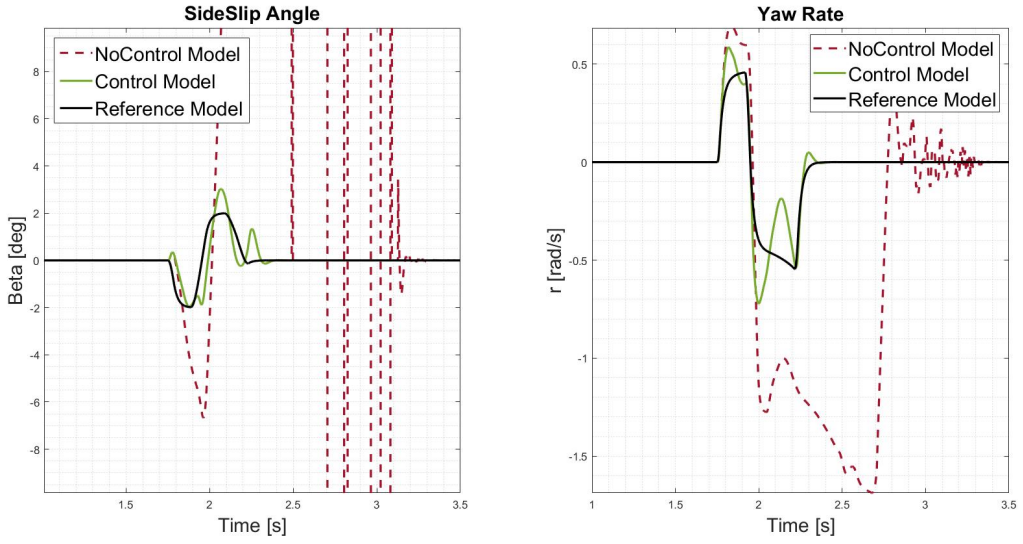

Fig. 11. Control operation in a SWD.

The plots show how the vehicle without the controller loses its stability and starts to spin.

In the Fig. 11 the reference, the controlled and the no-controlled model are shown. It is clearly visible that the vehicle checked is able to follow the side-slip angle and yaw rate values given by the reference and is able to maintain stability. The wheels braked are the outer front ones. In fact, the uncontrolled vehicle shows an oversteering behaviour

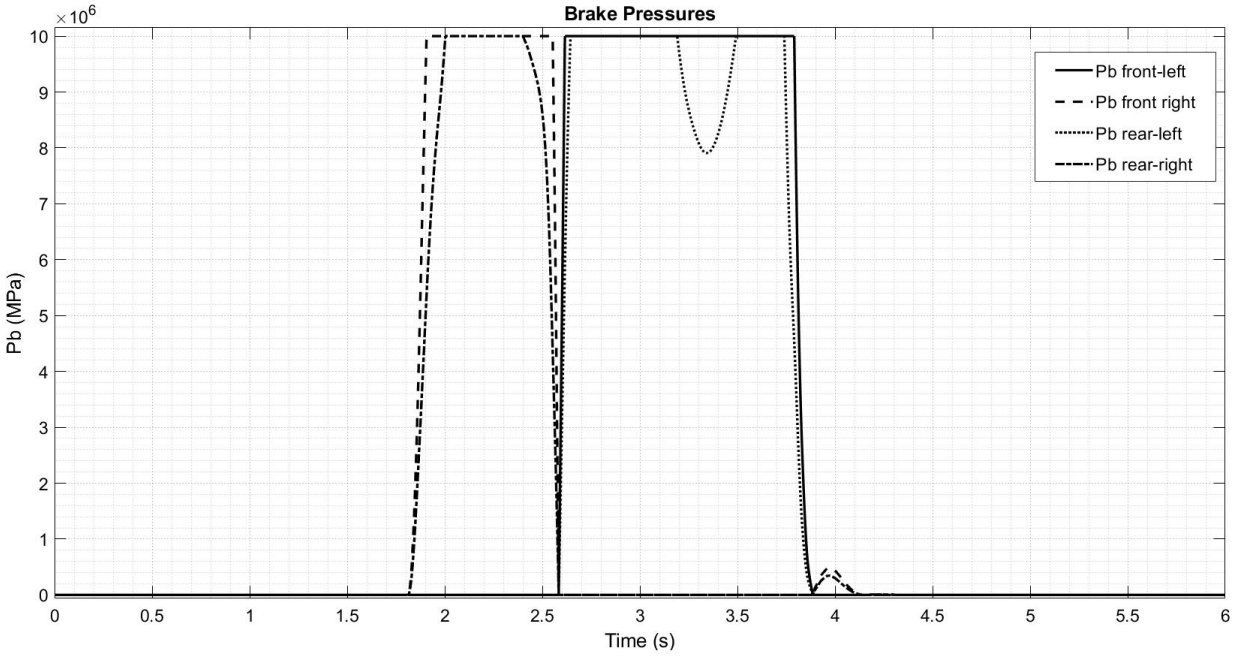

Fig. 12. Braking Pressures in a SWD.

that ends with its spin. Fig.13 shows the trajectory of the vehicle with the controller and without the controller. It is possible to note how the uncontrolled vehicle can't finish the manoeuvre and loses its stability. Instead, the controller ensures stability and control also at limit of handling condition.

9. Conclusions

The paper presents a stability vehicle controller based on a trajectory tracking LQR. The use of this controller involves the schematization of the vehicle as a single-track model and two phases of law controller, a feedback and a feedforward. Standard LQRs are usually optimized off-line with a known reference trajectory. The LQR presented in this study is optimized on-line ensuring that the dynamic model adapts to different longitudinal speeds and different lateral engage that the car faces during its motion. In addition, the reference model is expressed in a dynamic form within the controller, becoming a states of it: thus being able to be updated every time step. So, a yaw moment input is given to the vehicle continuously in order to follow the reference behaviour. However, the vehicle receives the total input as signal pressures that each brake actuator has to give to the wheels. The pressure at each wheel depends on the input yaw moment sign and on the actual tyre's contact patch. If the control system detects that a positive yaw moment must be added to the vehicle, the brake logic splits this moment between the front and rear left wheels in proportion to the availability of longitudinal slip. Otherwise, if the the control system detects a negative yaw moment, the brake logic splits it between the right wheels.

This solution ensures the achievement of very good performances thanks to the possibility of use four actuators able to continuously work and optimally manage the individual pressures at the wheels. In fact, it is possible to implement the controller in a real time simulator and ensure a continuous interaction with innovative brake actuators. Tests show that this control results robust in different type of conditions, in steady-state manoeuvres and at limit of handling, for different longitudinal velocities and steering angles. These results ensure that the control system can be used in vehicle that operates at limit of handling whether they are driven by a human or a driver-less vehicle.

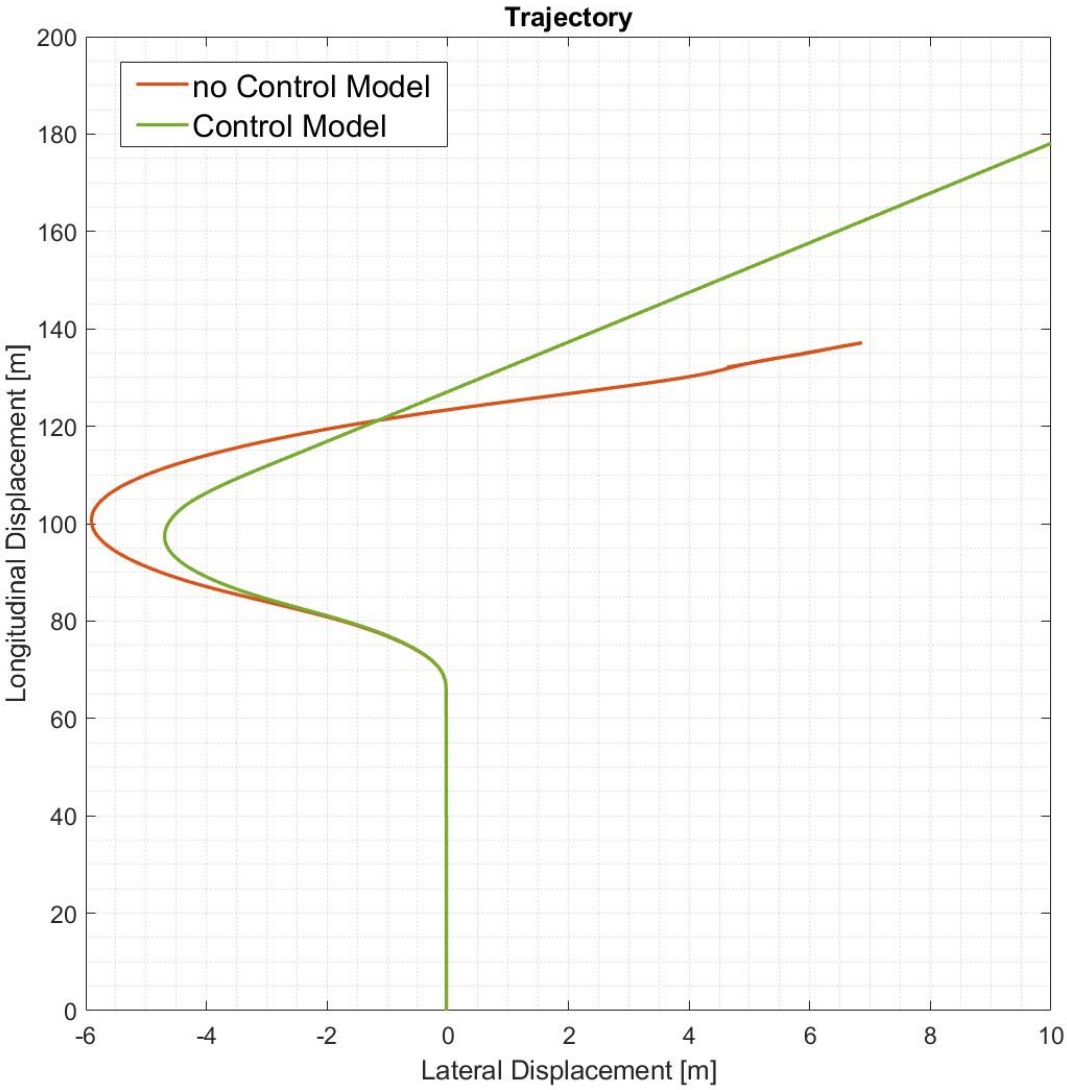

Fig. 13. Trajectory in a SWD.

References

Ataei, M., Khajepour, A., Jeon, S., 2019. Model Predictive Control for integrated lateral stability, traction/braking control, and rollover prevention of electric vehicles. In: Vehicle System Dynamics, pp. 1–25.

Barbarisi, O., Palmieri, G., Scala, S., Glielmo, L., 2009. LTV-MPC for Yaw Rate Control and Side Slip Control with Dynamically Constrained Differential Braking. In: European Journal of Control 15, pp. 468–479.

Bernard, J.E., Clover, C.L., 1995. Tire Modeling for Low-Speed and High-Speed Calculations. In: International Congress e Exposition.

Boada, B.L., Boada, M.J.L., Diaz, V., 2016. Vehicle sideslip angle measurement based on sensor data fusion using an integrated ANFIS and an Unscented Kalman Filter algorithm. In: Mechanical Systems and Signal Processing 72–73, pp. 832–845.

Dal Poggetto, V.F., Serpa, A.L., 2016. Vehicle rollover avoidance by application of gain-scheduled LQR controllers using state observers. In:Vehicle System Dynamics 54, pp. 191–209.

Du, X., Sun, H., Qian, K., Li, Y., Lu, L., 2010. A prediction model for vehicle sideslip angle based on neural network. In: 2010 2nd IEEE

International Conference on Information and Financial Engineering, pp. 451–455.
Falcone, P., Borrelli, F., Asgari, J., Tseng, H.E., Hrovat, D., 2007. Predictive Active Steering Control for Autonomous Vehicle Systems. In: IEEE Transactions on Control Systems Technology 15, pp.566–580.
Falcone, P., Eric Tseng, H., Borrelli, F., Asgari, J., Hrovat, D., 2008. MPC-based yaw and lateral stabilisation via active front steering and braking. In: Vehicle System Dynamics 46, pp. 611–628.
Jalali, M., Khosravani, S., Khajepour, A., Chen, S., Litkouhi, B., 2017. Model predictive control of vehicle stability using coordinated active steering and differential brakes. In: Mechatronics 48, pp. 30–41.
Johansen, T.A., Petersen, I., Kalkkuhl, J., Ludemann, J., 2003. Gain-scheduled wheel slip control in automotive brake systems. In: IEEE Transactions on Control Systems Technology 11, pp. 799–811.
Li, L., Jia, G., Chen, J., Zhu, H., Cao, D., Song, J., 2015. A novel vehicle dynamics stability control algorithm based on the hierarchical strategy with constrain of nonlinear tyre forces. In: Vehicle System Dynamics 53, pp. 1093–1116.
Li, L., Jia, G., Ran, X., Song, J., Wu, K., 2014. A variable structure extended Kalman filter for vehicle sideslip angle estimation on a low friction road. In: Vehicle System Dynamics 52, pp. 280–308.
Melzi, S., Sabbioni, 2011. On the vehicle sideslip angle estimation through neural networks: Numerical and experimental results. In: Mechanical Systems and Signal Processing 25, pp. 2005–2019.
Mosca, E., 1995. Optimal, predictive, and adaptive control, Prentice Hall information and system sciences series. In: Prentice Hall, Englewood Cliffs, N.J.
Novi, T., Capitani, R., Annicchiarico, C., 2016. An integrated ANN-UKF vehicle sideslip angle estimation based on IMU measurements. In: Proceedings of the Institution of Mechanical Engineers, Part D: Journal of Automobile Engineering, 233(7), pp. 1864–1878.
Ohno, H., Suzuki, T., Aoki, K., Takahasi, A., Sugimoto, G., 1994. Neural network control for automatic braking control system. In: Neural Networks 7, pp. 1303–1312.
UN/ECE, 2015. Regulation No 13-H of the Economic Commission for Europe of the United Nations (UN/ECE) — Uniform provisions concerning the approval of passenger cars with regard to braking [2015/] 84.
van Zanten, A.T., n.d. Evolution of Electronic Control Systems for Improving the Vehicle Dynamic Behavior.
Zhu, B., Piao, Q., Zhao, J., Guo, L., 2016. Integrated chassis control for vehicle rollover prevention with neural network time-to-rollover warning metrics. In: Advances in Mechanical Engineering 8, pp. 13.